

# Palladium-Catalyzed Amination of Aryl Bromides and Aryl Triflates Using Diphosphane Ligands: A Kinetic Study

Yannick Guari, Gino P. F. van Strijdonck, Maarten D. K. Boele, Joost N. H. Reek, Paul C. J. Kamer, and Piet W. N. M. van Leeuwen\*<sup>[a]</sup>

**Abstract:**  $[\text{Pd}(\text{P}-\text{O}-\text{P})(\text{Ar})]^+$  complexes with ligands that have wide bite angles are active catalysts for the coupling of aniline derivatives with aryl triflates. Kinetic studies show that for these systems a fast equilibrium that involves coordination of the amine precedes the deprotonation, which is the rate-limiting step of the reaction. This reaction is faster for compounds with a smaller P–Pd–P angle. When halide salts are present, the base sodium *tert*-butoxide is activated and adds to the palladium complex. This rate-limiting step is preceded by a fast equilibrium that involves decoordination of the halide. The initial reaction rate is faster for compounds with a larger P–Pd–P angle. This is due to the closer proximity of the oxygen to the Pd center, and this assists in the dissociation of the halide.

**Keywords:** amination • homogeneous catalysis • kinetics • palladium • phosphanes

## Introduction

During the past five years, extensive research devoted to the development of palladium-catalyzed carbon-nitrogen bond formation has led to efficient systems that offer considerable advantages over the classical methods (i.e. nonactivated substrates can be used, and neither highly polar solvents nor severe reaction conditions are required).<sup>[1]</sup> In the search for ligands that provide more active catalysts, improvements have recently been made by using bidentate phosphane,<sup>[2]</sup> aminophosphane,<sup>[3]</sup> and bulky electron-rich phosphane<sup>[4]</sup> ligands. The elegant work of both Hartwig and Buchwald has elucidated part of the mechanism of the amination reactions. These studies focused on monophosphane Pd species and *cis* chelating diphosphane Pd species by using catalysts prepared in situ.

Possible catalytic pathways for the amination of aryl halides are depicted in Scheme 1. The catalytic cycle starts with the oxidative addition of an aryl halide to  $[\text{Pd}(\text{P}-\text{P})]^0$  to give

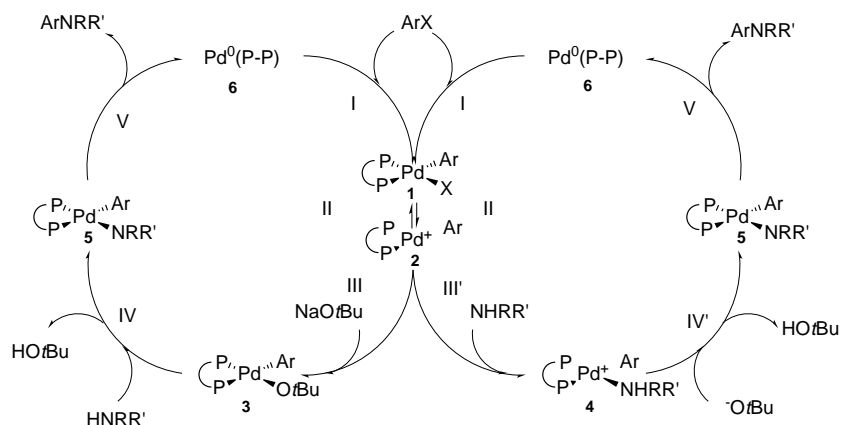
complex  $[\text{Pd}(\text{PP})(\text{Ar})(\text{X})]$  (**1**) (step I). This complex can react with sodium *tert*-butoxide to form complex **3**. The formation of  $[\text{Pd}(\text{PP})(\text{OR})(\text{Ar})]$  (**3**) could proceed either by an associative or a dissociative (steps II and III) pathway. Since a hemilabile terdentate ligand stabilizes the cationic intermediate **2**, the dissociative mechanism could be preferred with the use of a potentially terdentate ligand. Reaction of **3** with the amine (step IV) will give the amido complex **5**. Reductive elimination of the product (step V) will regenerate the active intermediate **6**.

Alternatively, complex  $[\text{Pd}(\text{PP})(\text{Ar})]^+$  (**2**) could react with the amine (step III') to afford complex **4**. Deprotonation by the base (step IV') will afford the amido complex **5**, which again will undergo reductive elimination. If the neutral complex **1** reacts with the amine, a similar pathway can be obtained that involves a neutral pentacoordinated Pd(amine) species and an anionic pentacoordinated amido complex. Oxidative addition of aryl triflates will directly lead to the formation of cationic complex **2**.

Hartwig proposed a catalytic cycle for *cis* chelating diphosphane Pd catalysts in the amination of aryl halides.<sup>[5]</sup> In this catalytic cycle, oxidative addition of an aryl halide to  $[\text{Pd}(\text{P}-\text{P})]^0$  (step I) gives complex **1**,  $[\text{Pd}(\text{PP})(\text{Ar})(\text{X})]$ . Successive reactions with base (step II) and amine (step III) lead to amido complex **5**, after which reductive elimination of  $\text{ArNRR}'$  regenerates  $[\text{Pd}(\text{P}-\text{P})]^0$  (**6**). An alternative route, suggested by Buchwald, is based on the reaction of the amine with  $[\text{Pd}(\text{PP})(\text{Ar})(\text{X})]$  (**1**) to afford a pentacoordinate complex followed by deprotonation by the base to form the amido complex.<sup>[6]</sup>

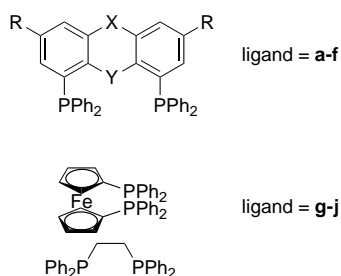
[a] Prof. Dr. P. W. N. M. van Leeuwen, Dr. Y. Guari  
Dr. G. P. F. van Strijdonck, Dr. M. D. K. Boele  
Dr. J. N. H. Reek, Dr. P. C. J. Kamer  
Institute of Molecular Chemistry  
Department of Inorganic Chemistry, Universiteit van Amsterdam  
Nieuwe Achtergracht 166, 1018 WV Amsterdam (The Netherlands)  
Fax: (+31)20-5256456  
E-mail: pwnm@anorg.chem.uva.nl

Supporting information for this article is available on the WWW under <http://www.wiley-vch.de/home/chemistry/> or from the author. Plots that show the zeroth-order dependency of the remaining reagents are available as Supporting information.



Scheme 1. Possible pathways for the palladium-catalyzed carbon-nitrogen bond formation.

We previously described the use of the ligand Xantphos (9,9-dimethyl-4,6-bis(diphenylphosphano)xanthene, **e**) in the palladium-catalyzed amination of aryl bromides.<sup>[7]</sup> With Pd(OAc)<sub>2</sub> as the Pd source, this system establishes the efficient and selective coupling of aryl bromides with primary aliphatic amines, anilines, and cyclic secondary amines. The use of DPEphos (bis[2-(diphenylphosphano)phenyl]ether, **a**) as a ligand was reported to be less general and less efficient than other Xantphos-type ligands (see Scheme 2).

Scheme 2. Structures of phosphane ligands: **a** = DPEphos, X = H, H, Y = O, and R = H; **b** = Homoxantphos, X = CH<sub>2</sub>CH<sub>2</sub>, Y = O, and R = H; **c** = Sixantphos, X = Si(CH<sub>3</sub>)<sub>2</sub>, Y = O, and R = H; **d** = Thioxantphos, X = S, Y = O, and R = CH<sub>3</sub>; **e** = Xantphos, X = C(CH<sub>3</sub>)<sub>2</sub>, Y = O, and R = H; **f** = Thioxantphos, X = C(CH<sub>3</sub>)<sub>2</sub>, Y = S, and R = H; **g** = dppf; **h** = dppe; **i** = PPh<sub>3</sub>; **j** = P(*o*-tolyl)<sub>3</sub>.

Recently, we have prepared a series of [palladium(II)-(*p*-C<sub>6</sub>H<sub>4</sub>CN)] complexes with different diphosphane ligands (see Scheme 3). They have been fully characterized and details will be presented elsewhere.<sup>[8]</sup>

The structures of complexes **1a**, **b**, and **g** show a chelating phosphane that accommodates a common *cis* coordination mode.<sup>[9]</sup> Complexes **1c–e**, however, show a *trans* coordination mode. We assume that the oxygen is forced into proximity of the Pd center by the *trans* coordination mode of the phosphane groups, and this leads to a weak Pd–O interaction. In solution, compounds **1c–e** show a *cis/trans* isomerization. Furthermore, cationic complexes [Pd(PP)(*p*-C<sub>6</sub>H<sub>4</sub>CN)]<sup>+</sup> **2c–f** have been synthesized and fully characterized. These complexes adopt an almost square planar geometry around the metal center with the ligand acting as a “pincer”, and the phosphane groups are in *trans* orientation, and the oxygen

atom is coordinated to the metal center. Isolation of *cis* complexes **2'a**, **b**, and **g** required acetonitrile.

In order to interpret the ligand effects and to determine the origin of the difference in performance found for DPEphos and Xantphos ligands in the palladium-catalyzed amination reaction, we used complexes **1** and **2** in an amination reaction. A kinetic study was performed to gain further insight into the details of the catalytic cycle.

## Results

As a model reaction we used the coupling of 2-methoxyaniline (*o*-anisidine) with bromobenzene and phenyl triflate. Sodium *tert*-butoxide was used as a base and toluene as a solvent. Since it is known that dba (dibenzylidene acetone) can interfere with the oxidative addition<sup>[10]</sup> and we wanted to exclude any rate effect of the formation of a catalytic species from a precatalyst (e.g. reduction of Pd<sup>II</sup> to Pd<sup>0</sup>), we used compounds **1** and **2**, as proposed intermediates of the catalytic cycle, rather than using in situ prepared catalysts from [Pd<sub>2</sub>(dba)<sub>3</sub>] or Pd(OAc)<sub>2</sub> and ligand.

**Catalysis with neutral complexes (1):** In Table 1, the results for the arylation of 2-methoxyaniline catalyzed by compounds **1** at room temperature are shown. In all reactions, only the monoarylated product was observed. Under these reaction conditions, the Pd<sup>II</sup> compounds with ligating monophosphanes (entry 8 and 9) show no conversion. Also for [Pd(dppe)(Ar)(Br)] (1,2-bis(diphenylphosphano)ethane) (**1h**), no activity was observed (entry 7). The compounds with the ligands enforcing a *cis* coordination mode gave low conver-

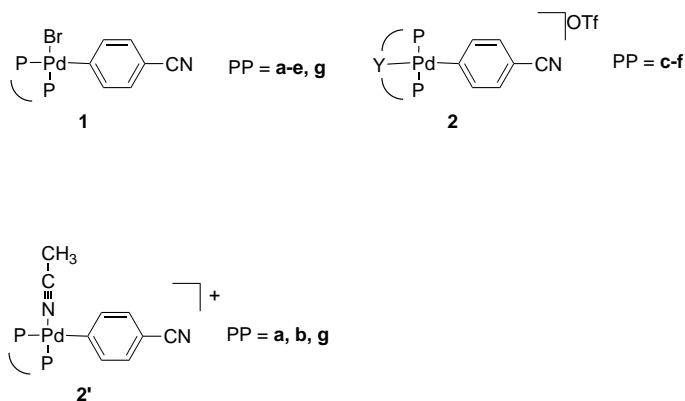
Scheme 3. [Pd<sup>II</sup>(PP)(*p*-C<sub>6</sub>H<sub>4</sub>CN)] complexes (PP): **1a** = DPEphos; **1b** = Homoxantphos; **1c** = Sixantphos; **1d** = Thioxantphos; **1e** = Xantphos; **1g** = dppf; **2c** = Sixantphos, and Y = O; **2d** = Thioxantphos, and Y = O; **2e** = Xantphos, and Y = O; **2f** = Thioxantphos, and Y = S; **2'a** = DPEphos; **2'b** = Homoxantphos; **2'g** = dppf.

Table 1. Catalytic amination of bromobenzene at 25 °C with complexes **1**.<sup>[a]</sup>

complex	TOF <sub>ini</sub> <sup>[b]</sup> [mol mol <sup>-1</sup> h <sup>-1</sup> ]	conversion <sup>[c]</sup> [%]	natural bite angle <sup>[d]</sup>
1 <b>1a</b>	22	3	102
2 <b>1b</b>	27	11	102
3 <b>1c</b>	80	40	109
4 <b>1d</b>	86	47	110
5 <b>1e</b>	140	96	111
6 <b>1g</b>	0	1	96
7 <b>1h</b>	0	0	85
8 <b>1i</b> <sup>[e]</sup>	0	0	–
9 <b>1j</b> <sup>[f]</sup>	0	0	–

[a] Conditions: see Experimental Section. [b] TOF<sub>ini</sub> is the amount of product formed per molPd per hour after six minutes. [c] Based on bromobenzene (*o*-anisidine and product yield give similar results) after 1 h. [d] Values taken from ref. [11]. For a recent review about bite angles, see ref. [11]. [e] [Pd(PPh<sub>3</sub>)<sub>2</sub>(*p*-C<sub>6</sub>H<sub>4</sub>CN)(Br)] was used. [f] Dimeric compound [Pd(P(*o*-tolyl)<sub>3</sub>)(*p*-C<sub>6</sub>H<sub>4</sub>CN)(*μ*-Br)]<sub>2</sub> was used.

sions (entries 1, 2, and 6), whereas the complexes with wide P–Pd–P angles showed excellent conversions after one hour under these very mild conditions. The observed reaction rates for these ligands follow the order **c** < **d** < **e**.

**Catalysis with cationic complexes (2):** In Table 2, the results of the reaction between 2-methoxyaniline and phenyl triflate catalyzed by the cationic complexes **2** are presented. The trend observed for the reaction rate with the neutral complexes is reversed. Compound **2f**, which only exists in the cationic form due to the strong coordination of the soft sulfur atom,<sup>[8]</sup> is not active in the amination reaction under the conditions tested.

Table 2. Amination of phenyl triflate at 25 °C with complexes **2**.<sup>[a]</sup>

complex	TOF <sub>ini</sub> <sup>[b]</sup> [mol mol <sup>-1</sup> h <sup>-1</sup> ]	conversion <sup>[c]</sup> [%]	yield [%]
1 <b>2c</b>	222	76	50
2 <b>2d</b>	200	66	44
3 <b>2e</b>	160	50	35
4 <b>2f</b>	0	0	0

[a] Conditions: see Experimental Section. [b] TOF<sub>ini</sub> is the amount of product formed per molPd per hour after six minutes. [c] Based on phenyl triflate after 1 h.

The conversion of phenyl triflate is higher than the conversion of the amine and the product yield. This is due to reaction of sodium *tert*-butoxide with phenyl triflate that forms sodium phenoxide and butyl triflate. This butanolysis reaction has been observed before.<sup>[12]</sup> This cleavage of triflates can be avoided by the slow addition of the aryl triflate or the use of a non-nucleophilic base. The latter solution, however, is not generally applicable, since for some aminations, the reaction only proceeds when sodium *tert*-butoxide is used. Since under standard conditions the butanolysis reaction is slower than the amination reaction (less than 3% after six minutes), the kinetics of the cationic reaction is only influenced at high conversions.

The cationic complexes [Pd(PP)(Ar)(CH<sub>3</sub>CN)]<sup>+</sup> (**2'**) showed no conversion in the amination reaction under the conditions employed. In general, addition of acetonitrile to amination reaction mixtures inhibits the formation of product.

**Effect of halide salts:** Since during the reaction of bromobenzene with 2-methoxyaniline sodium bromide is formed, we tested the effect of the halide salt concentration on the activity of compound **2e** in the amination of phenyl triflate. Table 3 shows that the activity of the catalyst in the model reaction is largely dependent on the concentration of halides present. In general, the initial activity was higher when halide salt was

Table 3. The effect of added halide salts in the amination of phenyl triflate at 25 °C with complex **2e**.<sup>[a]</sup>

	[additive] [mM]	TOF <sub>ini</sub> <sup>[b]</sup> [mol mol <sup>-1</sup> h <sup>-1</sup> ]	yield <sup>[c]</sup> [%]
1	no	160	35
2	3.9 (NaCl)	290	59
3	27.4 (NaCl)	257	42
4	165.6 (NaCl)	260	76
5	0.5 (Bu <sub>4</sub> NBr)	384	79
6	2.0 (Bu <sub>4</sub> NBr)	355	67
7	29.4 (Bu <sub>4</sub> NBr)	640	68
8	200 (Bu <sub>4</sub> NBr)	624	49
9	0.8 (Bu <sub>4</sub> NI)	169	72
10	2.5 (Bu <sub>4</sub> NI)	224	75
11	47 (Bu <sub>4</sub> NI)	238	77
12	276 (Bu <sub>4</sub> NI)	208	74

[a] Conditions: see Experimental Section. [b] TOF<sub>ini</sub> is the amount of product formed per molPd per hour after six minutes. [c] Based on phenyl triflate after 1 h.

added. At higher salt concentrations, the initial reaction rate slowed down again. The effect was most prominent for the use of bromide. The values found for the yield after one hour were obscured by the drop in base concentration due to the butanolysis reaction.

The halide salt concentration has a dramatic effect on the reaction rate and kinetics of the amination of bromobenzene. Figure 1 shows a nonlinear first-order plot of the aryl halide concentration in the reaction with 2-methoxyaniline catalyzed by **1e**. From these results, it is clear that the reaction rate actually increases during the course of the reaction. Addition of an excess of tetrabutylammonium bromide (50 equivalents relative to complex **1e**) provided a linear first-order plot.

**Kinetic experiments:** Since the data for the amination of phenyl triflate were obscured by the cleavage reaction, we were not able to analyze the reaction profile. To be able to determine the rate-limiting step, we performed some single-point kinetic experiments. The observed initial rate constants, *k*<sub>ini</sub>, for reactions with different initial concentrations of Pd<sup>II</sup> complex, 2-methoxyaniline, bromobenzene or phenyl triflate, and sodium *tert*-butoxide were determined. The concentration of the other reactants was kept constant by using them in large excess.

**Neutral complexes:** Kinetic data for the reaction between 2-methoxyaniline and bromobenzene catalyzed by complexes **1a** and **1e** were obtained by monitoring the formation of product by GC. Since complex **1a** is not very active at 25 °C, the reactions were performed at 40 °C.

The observed initial rate constant is independent of the concentration of 2-methoxyaniline (0.09–0.74 M) and the

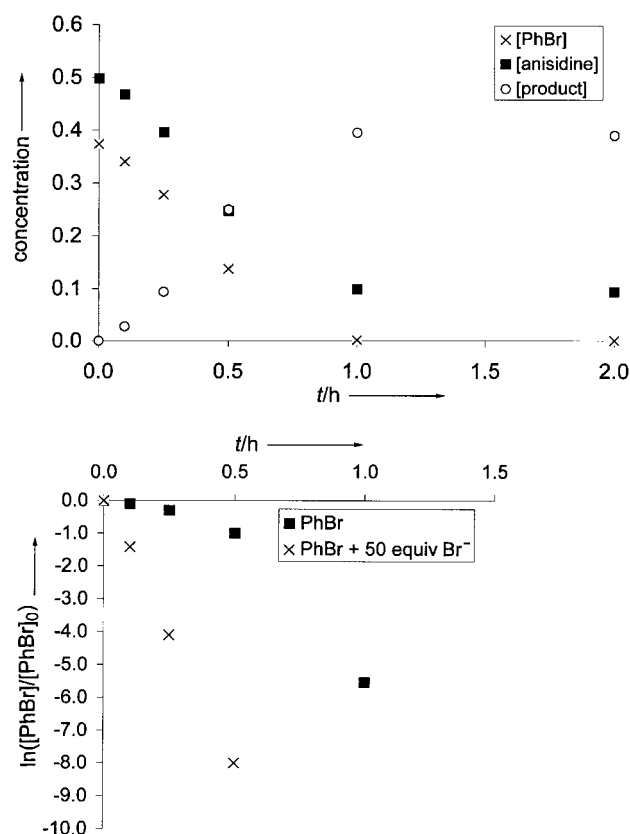


Figure 1. Plot of concentration versus time for the reaction of 2-methoxyaniline with bromobenzene catalyzed by complex **1e** (top) and first-order plot of the decay of bromobenzene with  $\text{Br}^-$  (50 equiv) and without additional  $\text{Bu}_4\text{NBr}$  (bottom).

concentration of bromobenzene (0.23–0.62 M). Figure 2 shows the linear dependence of  $k_{\text{ini}}$  on the sodium *tert*-butoxide concentration (0–0.65 M). The reaction rate increases approximately linearly with the square root of the

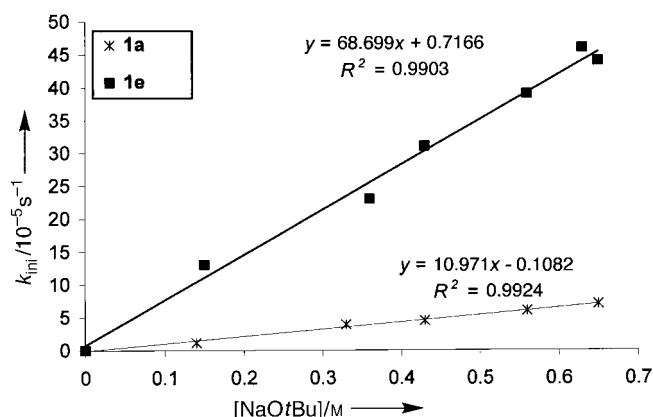


Figure 2. Plot of the  $k_{\text{ini}}^{[a]}$  versus  $[\text{NaOtBu}]$  for the reaction of 2-methoxyaniline with bromobenzene in toluene at 313 K catalyzed by complexes **1e** and **1a**.<sup>[b]</sup> [a] Measured after six minutes. [b] For experimental details: see Experimental Section.

palladium concentration (0–6.77 mM, see Figure 3). No formation of palladium black was observed under the conditions used.

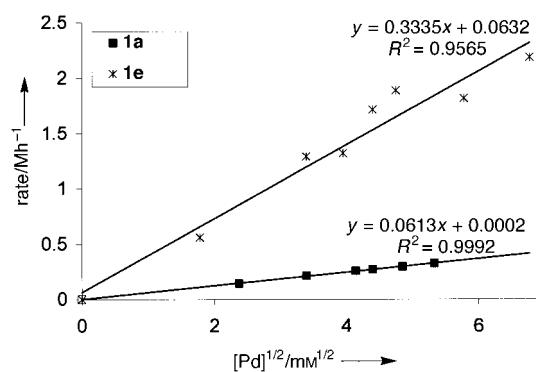


Figure 3. Plot of the rate<sup>[a]</sup> versus  $[\text{Pd}]^{1/2}$  with **1e** and **1a** for the reaction of 2-methoxyaniline with bromobenzene in toluene at 313 K.<sup>[b]</sup> [a] rate =  $d[\text{product}]/dt$ , measured after six minutes. [b] For experimental details: see Experimental Section.

**Effect of halide:** Kinetic experiments with **1e** as the catalyst in the presence of 50 equivalents of tetrabutylammonium bromide (in relation to palladium) showed a first-order dependency on the palladium concentration (0–4.15 mM,  $T=298$  K, see Figure 4).

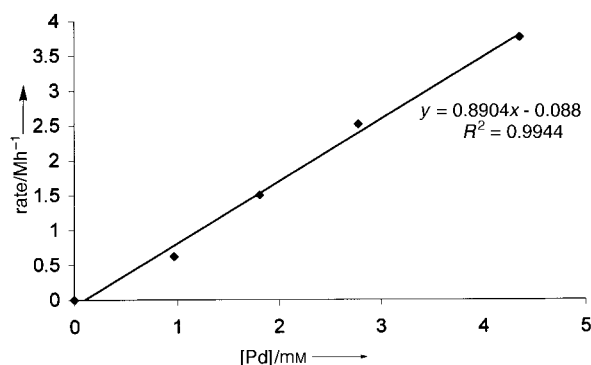


Figure 4. Plot of the rate<sup>[a]</sup> versus  $[\text{Pd}]$  for the reaction of 2-methoxyaniline with bromobenzene in toluene at 298 K catalyzed by **1e** in presence of 50 equivalents of tetrabutylammonium bromide.<sup>[b]</sup> [a] rate =  $d[\text{product}]/dt$ , measured after six minutes. [b] For experimental details: see Experimental Section.

**Cationic complexes:** With complex **2e**, the reaction rate increases linearly with the palladium concentration (0–4 mM, see Figure 5). This reaction shows an approximate first-order in 2-methoxyaniline and sodium *tert*-butoxide (see Figure 6), but the reaction rate is independent of the aryl triflate concentration.

**NMR experiments:** In the  $^{31}\text{P}\{^1\text{H}\}$ NMR spectrum of  $[\text{Pd}(\text{Xantphos})(p\text{-C}_6\text{H}_4\text{CN})(\text{Br})]$  (**1e**) in chloroform, a singlet was observed at  $\delta=9.4$ , whereas the cationic compound  $[\text{Pd}(\text{Xantphos})(p\text{-C}_6\text{H}_4\text{CN})\text{OTf}]$  (**2e**) showed a singlet at  $\delta=18.2$ . A mixture of **1e** and **2e** resulted in a broad peak between  $\delta=9.4$  and 18.2. At lower temperatures (190 K), these peaks decoalesced to their initial positions. Addition of an excess of sodium *tert*-butoxide to this mixture gave rise to a signal at

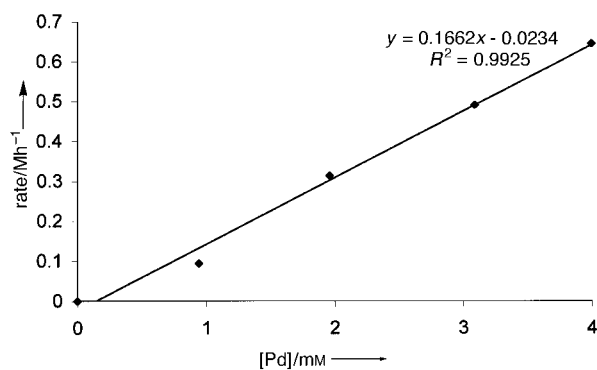


Figure 5. Plot of the rate<sup>[a]</sup> versus [Pd] for the coupling of 2-methoxyaniline with phenyltrifluoromethane sulfonate in toluene at 298 K catalyzed by **2e**.<sup>[b]</sup> [a] rate =  $d[\text{product}]/dt$ , measured after six minutes. [b] For experimental details: see Experimental Section.

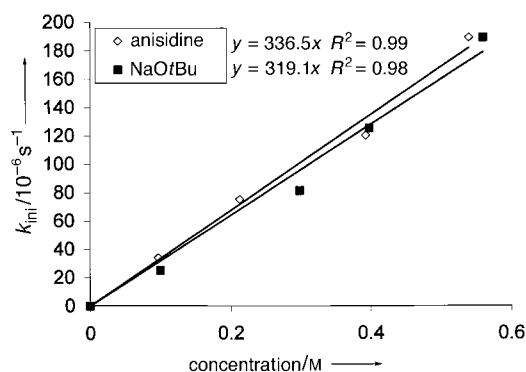


Figure 6. Plots of  $k_{\text{ini}}$ <sup>[a]</sup> versus [NaOtBu] and [*o*-anisidine] for the coupling of *o*-anisidine with phenyltrifluoromethane sulfonate in toluene at 298 K catalyzed by **2e**.<sup>[b]</sup> [a] Measured after six minutes. [b] For experimental details: see Experimental Section.

$\delta = 3.8$ . This signal was also observed when **1e** was reacted with *tert*-butoxide.

We studied the reaction by NMR spectroscopy under catalytic conditions to observe the resting state of the catalyst. To this end, a substoichiometric amount of sodium *tert*-butoxide was used in the reaction of 2-methoxyaniline with bromobenzene, with **1e** as the catalyst. At low temperatures, two broad signals at  $\delta = 9.4$  and 19.8 can be observed in  $^{31}\text{P}\{^1\text{H}\}$ NMR spectroscopy (see Figure 7). When the reaction takes place (at higher temperatures), these signals are still observed. Once the base had been consumed and the coupling reaction stopped, only the signal at  $\delta = 9.4$  was observed.

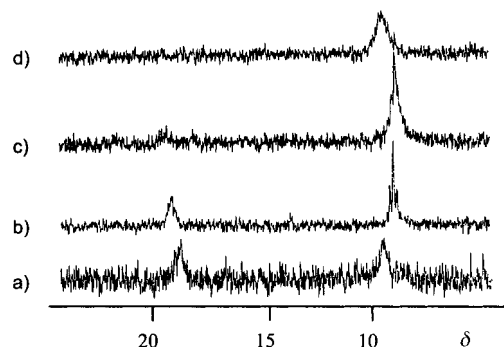


Figure 7.  $^{31}\text{P}\{^1\text{H}\}$ NMR spectra of a mixture of complex **1e**, bromobenzene, 2-methoxyaniline, and sodium *tert*-butoxide in  $[\text{D}_8]$ toluene recorded successively at a) 193 K, b) 273 K, c) 353 K, and d) 233 K.

## Discussion

From the kinetic results, obtained with the cationic complexes **2** and the neutral complexes **1**, we can conclude that the reaction pathway shifts to a different mechanism when halide salts are present.

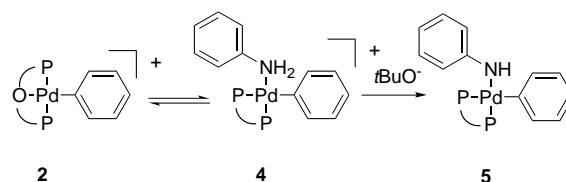
Hartwig et al. have reported the synthesis of palladium(II)-amido complexes and showed that for the C–N bond forming reductive elimination of monomeric phosphane ligated complexes two competing pathways are operative.<sup>[13]</sup> *Cis* chelated complexes of diphosphanes like dppe (1,1'-bis(diphenylphosphano)ferrocene) eliminate the product amine directly from a four-coordinate  $[\text{Pd}^{\text{II}}(\text{PP})(\text{amido})(\text{aryl})]$  complex. The kinetic data obtained in this study show that the reductive elimination is not the rate-limiting step, since the reaction rate shows a first-order dependence in base.

Recently, Buchwald reported that with  $\text{Pd}(\text{OAc})_2/\text{BINAP}$  (2,2'-bis(diphenylphosphano)-1,1'-binaphthyl) as precatalyst, the oxidative addition is the rate-limiting step.<sup>[6c]</sup> From the presented results ( $k_{\text{ini}}$  is independent of [bromobenzene] or [phenyl triflate]), however, we can conclude that by using our system the oxidative addition is not the rate-limiting step either. A similar result has been observed in a kinetic study dedicated to the palladium-catalyzed arylation of alkenes.<sup>[14]</sup>

**Catalysis with cationic complexes (2):** For the cationic compounds **2** we found the rate law expressed in Equation (1).

$$v = k[2][\text{NaOtBu}][o\text{-NH}_2\text{C}_6\text{H}_4\text{OCH}_3] \quad (1)$$

This equation is consistent with a mechanism in which the cationic starting compound (**2**) is in fast equilibrium with compound **4**. In the rate-limiting step, this compound is then deprotonated by the base to give compound **5** (see Scheme 4).



Scheme 4. Rate-limiting part of a proposed mechanism for the amination of aryl triflates.

Subsequently, the proposed pathway of reductive elimination and oxidative addition to give compound **2** is followed (see Scheme 1). The presented kinetic data, however, do not distinguish this pathway from a mechanism in which a pentacoordinated species  $[\text{Pd}(\text{PP})(\text{Ar})(\text{amine})(\text{OtBu})]$  is involved. An alternative explanation for the observed rate law would be a relatively slow reductive elimination from compound **5**, preceded by a fast equilibrium between **2**, **4**, and **5**. Since reductive elimination is faster with increasing bite angle, the observed bite angle<sup>[11]</sup> dependence (see Table 2) is not in agreement with this latter alternative mechanism.

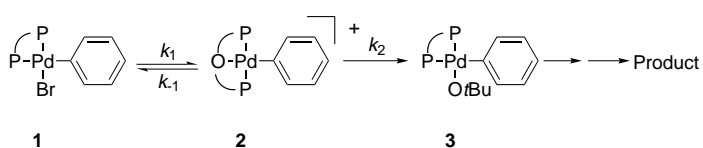
Going from a smaller bite angle (ligand **c**) to a larger bite angle (ligand **e**), the rate of the reaction decreases. We have

shown previously that compounds **1** exist as a mixture of *cis* and *trans* isomers in fast equilibrium.<sup>[8]</sup> Compounds with a larger natural bite angle prefer the *trans* isomer, whereas ligands with a smaller natural bite angle have a preference for the *cis* isomer. Ligands with a larger bite angle stabilize compounds **2**, and thus they shift the equilibrium between **2** and **4** towards the inactive intermediate **2**. Compound **2 f**, with a strongly coordinating sulfur atom, shows no activity, since the amine is not capable of replacing the sulfur. When acetonitrile is added to the reaction mixture, it inhibits amine coordination, and this results in a lower reaction rate.

With the monodentate tris(*o*-tolyl)phosphane ligand, a neutral Pd(amine) complex (viz. [Pd(P)(Br)(Ar)(amine)]) analogous to cationic complex **4** has been observed.<sup>[13]</sup> Coordination to palladium enhances the N–H acidity and after deprotonation, the anionic compound [Pd(P)(Br)(Ar)-(amido)]<sup>-</sup> was formed.<sup>[15]</sup>

**Catalysis with neutral complexes (1):** In contrast to the cationic complexes **2**, the use of neutral complexes **1** in the amination of bromobenzene shows that the reaction rate is independent of the amine concentration. From this we might conclude that the reaction follows a different pathway. Furthermore, at low conversion and thus low bromide concentration, the reaction rate shows a dependency on the palladium concentration which is of broken order (see Figure 3). At higher bromide concentrations, first-order dependence on the palladium concentration is recovered (see Figure 4).

**High halide concentration:** The kinetic data can be explained by the reaction sequence depicted in Scheme 5, if we consider a fast equilibrium that involves decoordination of the bromide. This equilibrium precedes the addition of the base, which is the rate-limiting step ( $k_2$ ), as shown in Scheme 5. Buchwald and co-workers have reported a series of *cis*-[Pd(PP)(OR)(Ar)] analogues of **3**, and this shows that these compounds are stable.<sup>[16]</sup>



Scheme 5. Proposed equilibrium between neutral compounds **1** and cationic compounds **2** in the amination of aryl bromides.

This dissociative mechanism gives the rate law expressed in Equation (2).

$$v = \frac{k_1 k_2 [\mathbf{1}] [\text{NaOtBu}]}{k_{-1} [\text{Br}^-]} \quad (2)$$

To verify the reaction sequence of Scheme 5, we carried out kinetic experiments with **1 e** as the catalyst in the presence of 50 equivalents of tetrabutylammonium bromide (with respect to the palladium concentration). Under these conditions, the rate law given in Equation (2) can be expressed as in

Equation (3), and this confirms the obtained first-order for the palladium concentration (Figure 4).

$$v = k[\mathbf{1}] [\text{NaOtBu}] \quad (3)$$

The mechanism depicted in Scheme 5 gives, according to Equation (2), a lower reaction rate at higher bromide concentrations. With *cis* chelating diphosphane Pd complexes, prepared in situ, the amination of aryl triflates was reported to be inhibited by added halides.<sup>[12]</sup>

Table 3 shows, however, that in this study halide salts accelerate the reaction dramatically. This effect levels off at higher halide concentrations. At even higher halide salt concentrations, the reaction is somewhat inhibited. These results can be explained in terms of two effects: an inhibitive effect as expected from Equation (2), and an accelerating effect due to the increased polarity of the solvent. Sodium *tert*-butoxide is likely to exist as a tight ion pair in toluene.<sup>[17]</sup> Addition of a salt could disrupt this ion pair, and this leaves a more activated butoxide. This effect is comparable to the rate enhancement obtained with addition of crown ether<sup>[18]</sup> and the higher activity of sodium *tert*-butoxide compared with lithium *tert*-butoxide.<sup>[19]</sup> The butoxide is activated and reacts with the cationic species to form the butoxide complex. Furthermore, addition of a salt increases the solvent polarity. This more polar solvent might shift the equilibrium towards the reactive, cationic species **2**.

The NMR spectra under catalytic conditions show the presence of starting material **1 e** ( $\delta = 9.4$ ), in exchange with cationic species (**2 e**). These results demonstrate that complexes **2** are true intermediates in the catalytic cycle. The reaction product of [Pd(PP)(Ar)(Br)] with sodium *tert*-butoxide, probably intermediate [Pd(PP)(Ar)(OtBu)] (**3**), could not be observed under catalytic conditions. This is as expected when this compound is formed in the rate-limiting step.

**Low halide concentration:** At low bromide concentration, the reaction rate shows a positive, broken, order in [Pd], a first order in sodium *tert*-butoxide, and a zeroth order in both 2-methoxyaniline and bromobenzene. The observed dependence on the palladium concentration might suggest that multiple equilibria, for example, between a dimeric species as the resting state and a monomeric species, which is the active intermediate, exist. From NMR spectroscopy, however, we can conclude that probably Pd dimers are not involved as the resting state, since under catalytic conditions only complexes **1 e** and **2 e** are observed.

As can be seen from this rate law, the halide formed in the initial stage of the reaction will retard the rate of catalysis. This decelerating effect will be more pronounced for more active systems, which generate free halide at a higher initial rate. Thus, experiments with high Pd loadings will give lower TOF<sub>min</sub>s, and therefore a broken order in [Pd] will be observed. At the same time, an increasing halide concentration will activate the base, as explained above. Therefore, at low halide concentrations opposing rate effects exist, which obscure the kinetics.

Additionally, at low halide concentration the reaction might also proceed by the alternative, cationic pathway (vide supra). As a result, the two routes can be operative simultaneously, and this results in complicated (i.e. nonunity order) kinetics with respect to [Pd]. However, since no dependence on amine concentration is observed, the role of the latter possibility is uncertain.

**Bite angle effect:** At low bromide concentrations, the initial reaction is faster for compounds with a larger P–Pd–P angle. This is due to the closer proximity of the oxygen to the Pd center; this assists the dissociation of the bromide and thus forces the equilibrium more to the active compounds **2**. Therefore, a higher concentration of complex **2** results in a higher overall reaction rate.

## Conclusion

A series of cationic and neutral [Pd(PP)(Ar)] complexes has been synthesized and used as catalysts in the amination of aryl triflates and aryl bromides. Kinetic studies show that for the cationic complexes, the rate-limiting step is the deprotonation of an Pd(amine) complex to form an amido complex. The amine complex is formed in a fast equilibrium from the starting cationic complex. In this reaction, the reaction rate is enhanced by smaller bite angles.

In the presence of halide salts, the sodium *tert*-butoxide is activated, and this results in a change of the reaction. The alternative pathway proceeds by the rate-determining formation of the Pd(alkoxide) complexes **3**. At higher concentrations of halides, the rate-enhancing effect of the salt levels off. This is due to a shift of the fast equilibrium between the active cationic species **2** and the inactive neutral compound **1** towards the latter, inactive species.

The higher rates obtained for complexes that contain ligands with larger bite angles can be correlated with a higher concentration of the corresponding active species **2**. Such an effect can be attributed to an additional driving force due to the ability of Xantphos to act as a terdentate ligand.

## Experimental Section

**General remarks:** All reactions were carried out under a nitrogen atmosphere using standard Schlenk techniques. All solvents were freshly distilled from standard drying agents under nitrogen before use. Phenyl triflate, bromobenzene, and *o*-anisidine were distilled before use. Sodium *tert*-butoxide, tetrabutyl ammonium bromide, tetrabutyl ammonium iodide, and sodium chloride were used as received.

<sup>31</sup>P NMR spectra (121.5 MHz, external 85% H<sub>3</sub>PO<sub>4</sub>, CDCl<sub>3</sub>) were recorded with a Bruker AMX-300 spectrometer. The product distribution was measured with an Interscience Mega2 apparatus equipped with a DB1 column (length 30 m, inner diameter 0.32 mm, film thickness 3.0 μm) and an FID detector.

The preparation and full characterization of the complexes will be described elsewhere.<sup>[8]</sup>

**Catalysis:** In a typical experiment, a Schlenk vessel, fitted with a septum and a magnetic stirring bar, was charged under nitrogen with the appropriate complex (0.0049 mmol), toluene (2 mL), decane (104 μL, 1 mmol) as internal standard, 2-methoxyaniline (135 μL, 1.2 mmol), and

bromobenzene (1.0 mmol) or phenyl triflate (1.0 mmol). When appropriate, tetrabutyl ammonium bromide, tetrabutyl ammonium iodide, or sodium chloride was added. The temperature was kept at 25 °C. Then, NaOtBu (135 mg, 1.4 mmol) was added (*t* = 0). The reaction was monitored by taking samples from the reaction mixture at specific intervals. Each sample was diluted with diethylether, washed with water, and the resulting organic fraction was analyzed by gas chromatography.

**Kinetic studies:** The kinetic studies were performed under the same conditions as described for the catalysis experiments, and the initial concentrations of one reagent were varied at a time. The total volume of the reaction was kept constant at 2.5 mL by adjusting the amount of toluene added.

**NMR experiment:** A frozen solution of complex **1e** (20 mg, 0.023 mmol), bromobenzene (157 mg, 1.0 mmol), 2-methoxyaniline (148 mg, 1.2 mmol), and sodium *tert*-butoxide (55.5 mg, 0.6 mmol) in [D<sub>8</sub>]toluene (2 mL) was allowed to melt before introduction in the NMR probe.

## Acknowledgements

We thank the Netherlands Ministry of Economic Affairs (IOP Katalyse) for support for this research.

- [1] a) J. F. Hartwig, *Angew. Chem.* **1998**, *110*, 2154–2177; *Angew. Chem. Int. Ed.* **1998**, *37*, 2046–2067; b) J. F. Hartwig, *Synlett.* **1997**, 329–340; c) J. P. Wolfe, S. Wagaw, J.-F. Marcoux, S. L. Buchwald, *Acc. Chem. Res.* **1998**, *31*, 805–818; d) B. H. Yang, S. L. Buchwald, *J. Organomet. Chem.* **1999**, *576*, 125–146.
- [2] a) B. C. Hamann, J. F. Hartwig, *J. Am. Chem. Soc.* **1998**, *120*, 7369–7370; b) J. P. Sadighi, M. C. Harris, S. L. Buchwald, *Tetrahedron Lett.* **1998**, *39*, 5327–5330.
- [3] D. W. Old, J. P. Wolfe, S. L. Buchwald, *J. Am. Chem. Soc.* **1998**, *120*, 9722–9723.
- [4] J. P. Wolfe, S. L. Buchwald, *J. Org. Chem.* **2000**, *65*, 1157–1167.
- [5] J. F. Hartwig, *Acc. Chem. Res.* **1998**, *31*, 852–860; b) G. Mann, J. F. Hartwig, *J. Am. Chem. Soc.* **1996**, *118*, 13109–13110.
- [6] a) J. P. Wolfe, S. Wagaw, S. L. Buchwald, *J. Am. Chem. Soc.* **1996**, *118*, 7215–7216; b) J. P. Wolfe, S. L. Buchwald, *Tetrahedron Lett.* **1997**, *38*, 5176–5185; c) J. P. Wolfe, S. L. Buchwald, *J. Org. Chem.* **2000**, *65*, 1144–1157.
- [7] Y. Guari, D. S. van Es, J. N. H. Reek, P. C. J. Kamer, P. W. N. M. van Leeuwen, *Tetrahedron Lett.* **1999**, *40*, 3789–3790.
- [8] M. A. Zuideveld, B. H. G. Swennenhuis, M. D. K. Boele, Y. Guari, J. N. H. Reek, P. C. J. Kamer, P. W. N. M. van Leeuwen, K. Goubitz, J. Fraanje, M. Lutz, A. L. Spek, G. P. F. van Strijdonck, unpublished results.
- [9] Reported X-ray crystal structures for complexes of the type [Pd(P–P)(X)(Ar)] with P–P = chelating phosphane, X = halide, and Ar = aromatic group: a) V. Dufaud, J. Thivolle-Cazat, J.-M. Basset, R. Mathieu, J. Jaud, J. Waisserman, *Organometallics* **1991**, *10*, 4005–4015; b) A. Bohm, K. Polborn, K. Sunkel, W. Beck, *Z. Naturforsch. B* **1998**, *53*, 448; c) W. A. Herrmann, C. Brossmer, T. H. Riermeier, K. Öfele, *J. Organomet. Chem.* **1994**, *481*, 97–108; d) I. R. Butler, L. J. Hobson, S. J. Coles, M. B. Hurthouse, K. M. Abdul Malik, *J. Organomet. Chem.* **1997**, *540*, 27–40; e) H. Trauner, P. le Floch, J.-M. Lefour, L. Ricard, F. Mathey, *Synthesis* **1995**, 717–726; f) J. M. Brown, J. J. Perez-Torrente, N. W. Alcock, H. J. Clase, *Organometallics* **1995**, *14*, 207–213.
- [10] C. Amatore, G. Broecker, A. Jutand, F. Khalil, *J. Am. Chem. Soc.* **1997**, *119*, 7215–7216.
- [11] P. W. N. M. van Leeuwen, P. C. J. Kamer, J. N. H. Reek, P. Dierkes, *Chem. Rev.* **2000**, *100*, 2741–2770.
- [12] J. Louie, M. S. Driver, B. C. Hamann, J. F. Hartwig, *J. Org. Chem.* **1997**, *62*, 1268–1273.
- [13] a) M. S. Driver, J. F. Hartwig, *J. Am. Chem. Soc.* **1997**, *119*, 8232–8245; b) F. Paul, J. Patt, J. F. Hartwig, *Organometallics* **1995**, *14*, 3030–3039; c) R. A. Widenhofer, S. L. Buchwald, *Organometallics* **1996**, *15*, 3534–3542; d) R. A. Widenhofer, S. L. Buchwald, *Organometallics*

- 1996**, *15*, 2755–2763; e) R. A. Widenhoefer, H. A. Zhong, S. L. Buchwald, *Organometallics* **1996**, *15*, 2745–2754.
- [14] G. P. F. van Strijdonck, M. D. K. Boele, P. C. J. Kamer, J. G. de Vries, P. W. N. M. van Leeuwen, *Eur. J. Inorg. Chem.* **1999**, 1073–1076.
- [15] J. Louie, F. Paul, J. F. Hartwig, *Organometallics* **1996**, *15*, 2794–3005.
- [16] R. A. Widenhoefer, H. A. Zhong, S. L. Buchwald, *J. Am. Chem. Soc.* **1997**, *119*, 6787–6795.
- [17] A. Jutand, A. Mosleh, *Organometallics* **1995**, *14*, 1810–1817.
- [18] J. P. Wolfe, S. L. Buchwald, *J. Org. Chem.* **1997**, *62*, 6066–6068.
- [19] J. Louie, J. F. Hartwig, *Tetrahedron Lett.* **1995**, 3609–3612.

Received: March 22, 2000 [F2380]